Macromolecules

ARTICLE

pubs.acs.org/Macromolecules

Versatile Superhydrophobic Surfaces from a Bioinspired Approach

Mélanie Wolfs, Thierry Darmanin, and Frédéric Guittard*

Université de Nice Sophia Antipolis, Equipe Chimie Organique aux Interfaces, Parc Valrose, 06108 Nice Cedex 2, France

Supporting Information

ABSTRACT: We report the surface wettability and morphology of conductive polymer films obtained by electrodeposition of poly(3,4-ethylenedioxythiophene) (i.e., PEDOT) derivatives containing an alkyl chain (PEDOTH$_n$ with n = 4, 6, 8, 10, and 12) or a phenyl (PEDOTPh) group in the 2-position. Even if the general approach in the literature is the use of highly fluorinated tail to reach superhydrophobic materials, we point out that versatile surfaces (from hydrophilic to superhydrophobic) can be obtained, in one step, without any fluorinated chemistry. Indeed, superhydrophobic surfaces were formed, using Bu_4NPF_6 and acetonitrile as electrolyte, by electrodeposition of PEDOT derivatives substituted with n-$C_{10}H_{21}$ and n-$C_{12}H_{25}$ chains, while the polymer films substituted with n-C_8H_{17} and n-C_6H_{13} were hydrophobic and those substituted with n-C_4H_9 and phenyl were hydrophilic. In the PEDOTH$_n$ series, the polymer films were structured only from n-C_8H_{17}, which proves the influence of long alkyl chains on both the surface wettability and the surface morphology due to the increase in polymer insolubility. By changing acetonitrile by dichloromethane, as solvent of electropolymerization, it is possible to produce smooth surfaces and as a consequence to determine the chemical and physical parts of the contact angles as well as roughness factors or air fractions following the Wenzel and Cassie−Baxter theories. By changing the salt for the electrodeposition, it also was possible to reach superhydrophobic surfaces even with short alkyl chains as well as without alkyl chains but using perfluorinated salts. In this work the mechanism to reach structured surfaces is also discussed. This work contributes to the formation of bioinspired superhydrophobic surfaces.

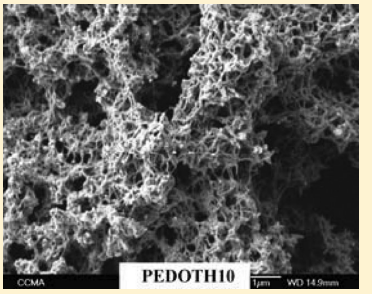

INTRODUCTION

The fabrication of biomimetic superhydrophobic surfaces is fast expanding due to the interest of both the scientific and industrial community.[1−3] Such surfaces were produced by combining surface structuration and hydrophobization.[4−6] The methods employed in the literature to fabricate structured surfaces can be divided in two global strategies: the top-down and the bottom-up approachs.[7−9] In all the tuned methods, the surface wettability control is crucial for the development of applied surfaces. For example, McCarthy et al. reported the fabrication of superhydrophobic surfaces, obtained by photolithography, with various wetting properties by controlling the dimensions of the posts but also their shape, their height, and the space between them.[7] However, such surfaces are expensive and difficult to produce.

Conductive polymers can also be used to form superhydrophobic surfaces using various strategies. First, conductive polymers could be deposited inside removable template to form nanostructured surfaces.[10−12] For example, Zhang et al. electrodeposited polyaniline inside the pores of an anodic aluminum oxide (AAO) template and obtained polyaniline nanowire film after dissolution of the template in alkaline media.[10] Another strategy involves the formation of conductive polymer micro/nanostructures in solution by chemical polymerization and using a self-assembled method following by their deposition on surfaces.[13−15] Hence, rambutan-like hollow spheres and dandelion-like microspheres of polyaniline were reported by the team of Wan and Jiang.[14,15] Jiang et al. also reported the deposition of polyaniline/polystyrene fibers by electrospinning.[16] Finally, structured conductive polymer can be deposited in a one-step process by electrochemical deposition.[17−24] This cost-effective, reproducible, and easy to implement process, used in the literature also to deposit metals and metal oxides,[25] allowed to produce surfaces of wettability depending on many parameters such as electrochemical parameters (doping agents, deposition charge, substrate, monomer concentration) or the monomer chemical structure (polymerizable core, presence of fluorocarbon or hydrocarbon chains of different length, presence of spacers). The incorporation of the hydrophobic part was introduced following three different ways: during a post-treatment,[24] using a hydrophobic supporting electrolyte (the counterion being incorporated in doped conductive polymers)[23] or a hydrophobic substituent was grafted to the monomer before polymerization.[17−22] Using the last way, surfaces of exceptional antiwetting properties and stability were elaborated by electropolymerization of substituted monomers including pyrrole, thiophene, and 3,4-ethylenedioxythiophene (EDOT) derivatives. Among all the monomers synthesized, the potential of EDOT derivatives was exceptional: superhydrophobicity achieved very quickly; various surface morphologies obtained by changing the chain length.[15]

Received: February 23, 2011
Revised: August 25, 2011
Published: November 09, 2011

Scheme 1. Studied Monomers (n = 4, 6, 8, 10, and 12)

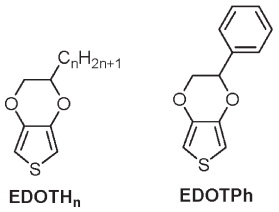

Scheme 2. Synthetic Way to the Monomers (n = 4, 6, 8, 10, and 12)

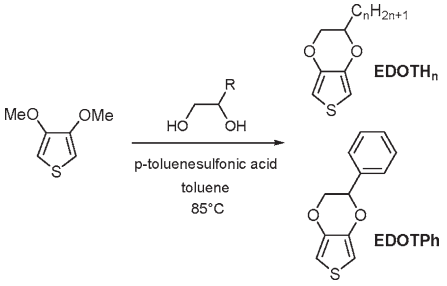

In order to achieve superhydrophobic properties, a general condition described in the literature involves the use of highly fluorinated tails (expensive materials) directly or as a post-treatment. However, many surfaces are able to repel water with contact angle above 150° and using only hydrocarbon materials such as hydrocarbon waxes.[26−29] The present paper points out it is possible to obtain versatile surfaces from hydrophilic to superhydrophobic without any fluorinated chemistry (bioinspired approach). Hence, we report the preparation and characterization of electrodeposited polymer films obtained from EDOT derivatives containing an alkyl or a phenyl substituent directly grafted on the 2-position (Scheme 1). The synthesis and the electrochemical characteristics of these monomers are reported in the Supporting Information. We report the surface morphologies and wettability of the polymer films electrodeposited in various electrochemical conditions on gold plates by scanning electron microscopy, optical profilometry, and contact angle measurements.

EXPERIMENTAL SECTION

Monomer Synthesis. All chemical products were purchased from Sigma-Aldrich. The synthesis of hydrocarbon monomers was inspired from the literature: transetherification of 3,4-dimethoxythiophene in toluene in the presence of *p*-toluenesulfonic acid and the corresponding diol.[30−32] The reaction was followed by a purification step by column chromatography (silica gel; eluent: cyclohexane/chloroform 4:1). The synthetic route to the monomers is represented in Scheme 2. The data of characterization are available in the Supporting Information.

Electrodeposition. The electropolymerization experiments were performed in anhydrous acetonitrile with 0.1 M tetrabutylammonium hexafluorophosphate and 0.01 M monomer using platinum working electrode for cyclic voltammetry analyses (determination of the monomer oxidation potential) or gold plates, purchased from Neyco, for polymer characterization, a glassy carbon counter electrode, and a SCE reference electrode. The monomer oxidation potentials were determined by cyclic voltammetry. A potential between 1.46 and 1.52 V vs SCE was measured for EDOTH$_n$ and EDOTPh. The study of the electropolymerization by multiple potential scanning is available in the Supporting Information. In order to study the surface properties, polymer films were electrodeposited by chronoamperometry using a potential slightly lower potential to that of the monomer oxidation.

Surface Characterization. The roughness parameters R_a and R_q were measured by a WYKO NT1100 optical profilometer fitted with a 0.5× field of view and a 50× objective. The area of each measurement was 182 μm × 239 μm. For each sample, the average values of three measurements at different positions were adopted as R_a and R_q parameters. The surface morphology was investigated with a JEOL 6700F microscope (SEM). The surface wettability was characterized by static contact angle of water and diiodomethane (2 μL droplet), while the dynamic contact angles were obtained with the tilted-drop method. In this method, the inclination of the surface on which a 6 μL water droplet is deposited gave the sliding angle (when the water droplet rolled off the surface) and the advanced and receding contact angles due to droplet deformation due to the inclination. The advanced and receding contact angles were taken just before the droplet rolled off the surface.

Table 1. Static Contact Angles of the Polymers Films (Salt: Bu_4NPF_6; $Q_s \approx 100$ mC/cm^2)

	CA_{water} [deg]	CA_{diiodo} [deg]
PEDOTH$_{12}$	158.6	0
PEDOTH$_{10}$	160.4	57.2
PEDOTH$_8$	133.9	88.1
PEDOTH$_6$	98.7	55.3
PEDOTH$_4$	81.3	49.5
PEDOTPh	83.6	0

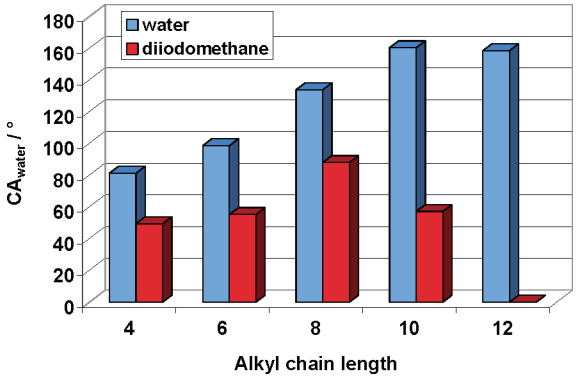

Figure 1. Static contact angles of water and diiodomethane in the PEDOTH$_n$ series as a function of the alkyl chain length.

RESULTS AND DISCUSSION

Surface Wettability. The surface hydrophobicity of the polymer surfaces was evaluated using 2 and 6 μL water droplets (γ_L = 72.8 mN/m) for the static and dynamic contact angles, respectively. The static contact angles are given in Table 1. While PEDOTH$_4$ was hydrophilic and PEDOTH$_6$ and PEDOTH$_8$ hydrophobic, PEDOTH$_{10}$ and PEDOTH$_{12}$ displayed superhydrophobic properties with contact angles (CA_{water}) close to 160° (Figure 1) and extremely low hysteresis and sliding angle (H_w = 2.4° and α_w = 1.5° for PEDOTH$_{12}$; H_w = 2.5° and α_w = 1.2° for PEDOTH$_{10}$). As a consequence, water droplets could easily bounce on these two surfaces. These values are very close to

dx.doi.org/10.1021/ma200430n |*Macromolecules* 2011, 44, 9286–9294

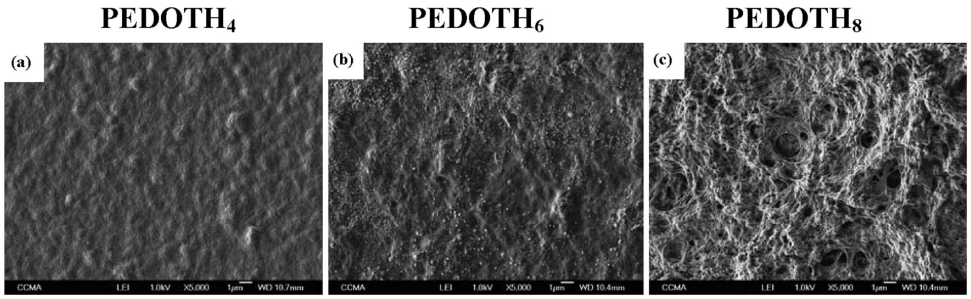

Figure 2. SEM images of (a) $PEDOTH_4$, (b) $PEDOTH_6$, and (c) $PEDOTH_8$ with a magnification of ×5000 (solvent: acetonitrile; salt: Bu_4NPF_6; Q_s = 200 mC/cm^2).

those obtained from electrodeposited fluorinated films,[17,18,20] which means a hydrocarbon chain is enough to reach superhydrophobic properties from EDOT series. Here, 10 methylene units in the hydrocarbon tail is a necessary condition to emphasize the hydrophobic properties of the film. These results can be correlated with the performances of hydrocarbon surfactants measured by the group of Eastoe.[33,34] Indeed, they observed that hydrocarbon surfactants can be designed to behave like fluorocarbon surfactants, especially with regard to CO_2 solubility/interfacial activity. By comparison, PEDOTPh was hydrophilic. Other measurements with diiodomethane, a liquid of surface tension lower than water, showed that none of these surfaces could repel this liquid but that, for this liquid probe, the best values were obtained with $PEDOTH_8$ (Table 1 and Figure 1). Indeed, an increase of the static contact angle of diiodomethane (CA_{diiodo}) with the alkyl chain length was observed from *n*-butyl to *n*-octyl and a decrease after. This behavior can be correlated not only to surface morphology of the films but also to the static contact angles of diiodomethane on "smooth surfaces". Indeed, CA_{diiodo} of $PEDOTH_4$ and $PEDOTH_6$ (smooth surfaces) is clearly below 90°, which means that the increase of surface roughness for such surfaces should decrease CA_{diiodo}, as observed for $PEDOTH_{12}$ ($CA_{diiodo} \approx 0°$), following Wenzel and Cassie–Baxter models.[4−6] However, CA_{diiodo} was close to 90° for $PEDOTH_8$. In this case, the surface morphology is probably responsible for this high CA_{diiodo}.

Surface Morphology and Roughness. SEM images are given in Figures 2 and 3 while the roughness parameters obtain by optical profilometry are gathered in Table 2. These data highlight the influence of the alkyl chain length on both the surface hydrophobicity and the surface morphology. Whereas $PEDOTH_4$ and $PEDOTH_6$ were not structured (Figure 2a,b), $PEDOTH_8$, $PEDOTH_{10}$, and $PEDOTH_{12}$ were micro- and/or nanostructured (Figures 2c and 3). More precisely, $PEDOTH_8$ films were porous while $PEDOTH_{10}$ and $PEDOTH_{12}$ were both micro- and nanostructured. The diameter of the porosities of $PEDOTH_8$ films may explain the good contact angle values measured with diiodomethane. Hence, it will be interesting to correlate the size of surface porosity and the contact angle with liquids of low surface tension as explained in fluorinated derivatives.[17] The surface morphology of $PEDOTH_{10}$ looked like an assembly of fibrils and that of $PEDOTH_{12}$ an assembly of thin needles, which explains their exceptional water-repellency properties. The surface morphology of $PEDOTH_8$ and $PEDOTH_{10}$ were close to surfaces observed in the previously reported PEDOT derivatives containing a methoxy−carbonyl as spacer between the hydrocarbon tail and the EDOT heterocycle,[20a] meaning that the spacer has not, in that case, a significant influence on the surface properties. Roughness analyses (Table 2) showed that the surface roughness increases from *n*-hexyl to *n*-decyl and decreases after as shown in Figure 3a,a′. The differences observed in the surface roughness for $PEDOTH_8$ and $PEDOTH_{10}$ can not explain their water-repellency properties. However, it is now establish that, during the electrodeposition of hydrophobic conductive polymer, CA_{water} usually increases with the surface roughness until to reach a plateau.[17,18] PEDOTPh was also structured as shown in Figure 4, but either the surface structuration was not sufficient or the polymer not intrinsically enough hydrophobic to reach superhydrophobic properties.

The measurements of the static contact angle of water and roughness parameters as a function of the deposition charge (Q_s) for the $EDOTH_n$ series showed that the roughness continuously increases with Q_s (the increase is very important for $PEDOTH_{10}$ and $PEDOTH_{12}$ due to the presence of surface micro/nanostructures) while the static contact angles of water quickly reach a plateau (Figures 5 and 6). Hence, for each surface morphology, a minimal surface roughness ($R_{a,min}$) can be introduced, which means that from this roughness value the surface becomes superhydrophobic and that the increase of roughness has just a slight effect on the water-repellent properties. The most influent physical parameter on the surface wettability is not the surface roughness, but the surface wettability is especially governed by the surface morphology as previously demonstrated in many publications.[35] From Figures 5 and 6 it can be deduced that $R_{a,min} \approx 200-300$ nm for $PEDOTH_{10}$ and $PEDOTH_{12}$. Moreover, superhydrophobic properties were reached from a smaller quantity of electrodeposited polymers, Figure 5 ($Q_s \approx 25$ mC/cm^2 for $EDOTH_{10}$ and 50 mC/cm^2 for $EDOTH_{12}$), than those observed from fluorinated series.[12,15]

Determination of the Chemical and Physical Part of Surface Water-Repellent Properties. To determine which parameters have the most influence on the surface wettability, it is very important to dissociate the chemical part (polymer + doping anions) from the physical one (roughness + morphology).

First, to measure the impact of the doping anions, the films were electrochemically reduced (−1 V vs SCE for 40 mn). The CA_{water} values of polymers as a function of their oxidation state are given in Figure 7. We determined a significant decrease (10°−20°) after reduction for $PEDOTH_4$, $PEDOTH_6$, and $PEDOTH_8$ (hydrophilic to hydrophobic state) but not for $PEDOTH_{10}$ and $PEDOTH_{12}$ (superhydrophobic state), which shows that the PF_6^- counterions could increase the hydrophobic properties. Therefore, it seems that, in the case of $PEDOTH_{10}$ and $PEDOTH_{12}$, the decrease in surface hydrophobicity after reduction was compensated by the physical part.

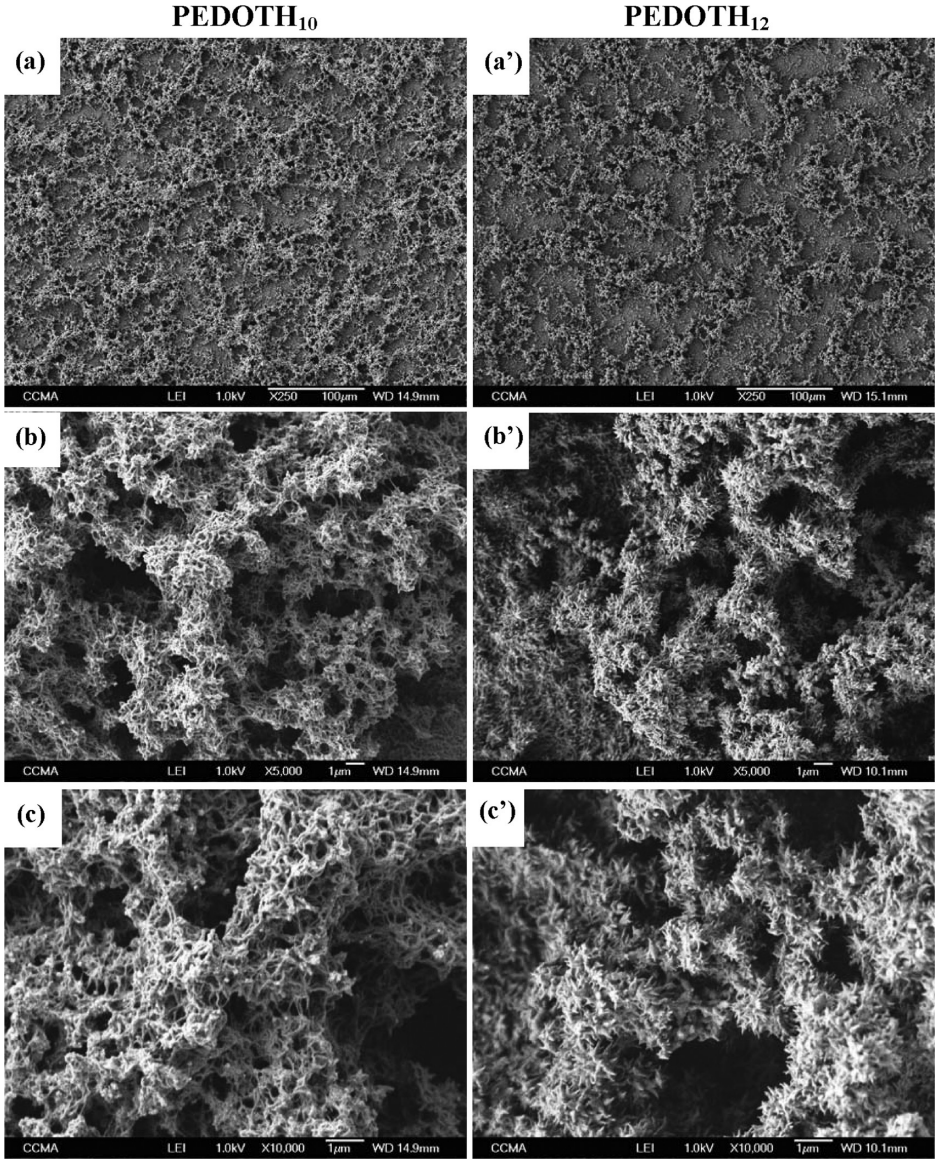

Figure 3. SEM images of $PEDOTH_{10}$ (with a magnification of (a) ×250, (b) ×5000, and (c) ×10000) and $PEDOTH_{12}$ (with a magnification of (a′) ×250, (b′) ×5000, and (c′) ×10000) (solvent: acetonitrile; salt: Bu_4NPF_6; Q_s = 200 mC/cm^2).

Table 2. Roughness Data for Q_s = 100 mC/cm^2

	roughness parameters	
polymers	R_a [μm]	R_q [μm]
$PEDOTH_{12}$	0.84	1.39
$PEDOTH_{10}$	1.31	1.81
$PEDOTH_8$	0.52	0.71
$PEDOTH_6$	0.16	0.24
$PEDOTH_4$	0.13	0.19
PEDOTPh	0.04	0.11

To determine the impact of the physical part (especially for $PEDOTH_8$, $PEDOTH_{10}$, and $PEDOTH_{12}$), it was necessary to produce smooth films with the same polymers. The first envisaged strategy was to solubilize the polymer and to deposit it for example by spin-coating. Unfortunately, all polymers were completely insoluble in various solvents. Hence, we chose to modify electrochemical parameters and more precisely the solvent used for the electrodeposition to directly form smooth surfaces. For these experiments, $EDOTH_{10}$ was chosen as monomer and acetonitrile was replaced by five other solvents of various polarities: propylene carbonate, benzonitrile, nitrobenzene, dichloromethane, and chloroform. The SEM images of the surfaces and the CA_{water} are given in Figures 8 and 9. Structured surfaces were obtained with all the highly polar solvents (acetonitrile, nitrobenzene, benzonitrile, and propylene carbonate) while the less polar solvents (dichloromethane and chloroform) gave smooth surfaces. The best nonwetting properties were obtained with acetonitrile while the surfaces obtained with benzonitrile displayed an unusual "petal-like" surface morphology.

Hence, it was possible to reach smooth surfaces (Figure 8d) for $PEDOTH_8$, $PEDOTH_{10}$, and $PEDOTH_{12}$ by replacing acetonitrile with dichloromethane in the electrodeposition process. The CA_{water} of these surfaces were 103.3°, 108.2°, and 110.5° for

dx.doi.org/10.1021/ma200430n |*Macromolecules* 2011, 44, 9286–9294

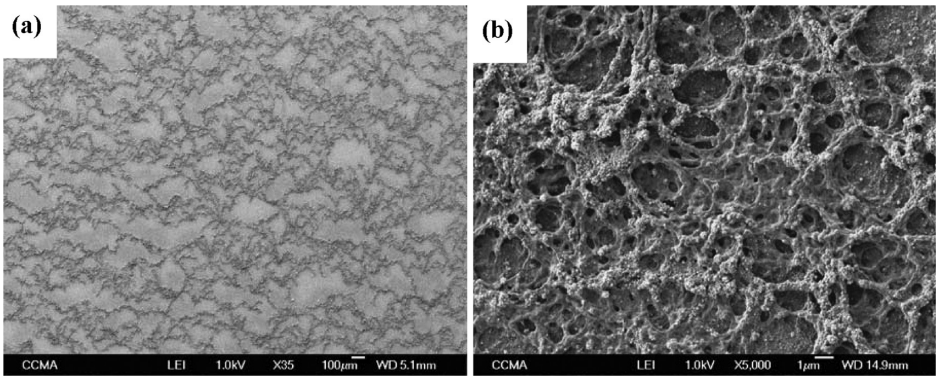

Figure 4. SEM images of PEDOTPh with a magnification of (a) ×35 and (b) ×5000 (solvent: acetonitrile; salt: Bu_4NPF_6; Q_s = 200 mC/cm^2).

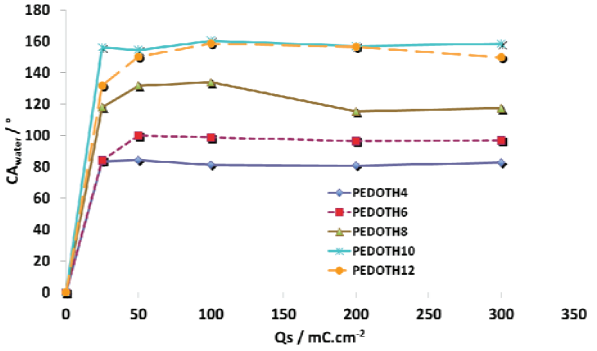

Figure 5. Static contact angles of water as a function of the deposition charge.

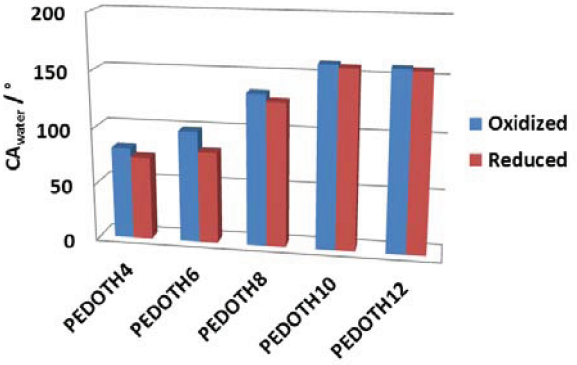

Figure 7. CA_{water} of polymers as a function of the oxidation state.

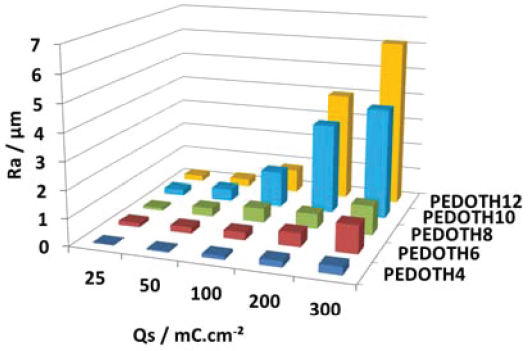

Figure 6. Mean arithmetic roughness (R_a) as a function of the deposition charge.

$PEDOTH_8$, $PEDOTH_{10}$, and $PEDOTH_{12}$, respectively, while the CA_{diido} were 47.8, 51.7° and 53.5°, confirming the effect of the surface porosity of $PEDOTH_8$ previously described. With the CA_{water} values, it was possible to deduce the physical part and as a consequence the chemical part of the polymer. The data are given in Table 3. From this table, it can be deduced that the physical part of the superhydrophobic $PEDOTH_{10}$ and $PEDOTH_{12}$ films represents about 30−35% while the doping anions only 1−2%.

The determination of contact angles on the corresponding smooth surfaces can only be used to determine the roughness factor (r) or air fraction (f_a) following the relation of Wenzel ($\cos CA = r \cos CA_{smooth}$)[4] and Cassie−Baxter ($\cos CA = (1 - f_a) \cos CA_{smooth} - f_a$),[5,6] respectively. Hence, for $PEDOTH_8$, electrodeposited in Bu_4NPF_6/acetonitrile, it can be supposed that a water droplet deposited on it, is close to a "Wenzel state", and that $r = \cos(133.9)/\cos(103.3) = 3.01$. This value was not sufficient to reach superhydrophobic surface properties. In the case of $PEDOTH_{10}$ and $PEDOTH_{12}$, the water droplet is close to a "Cassie−Baxter state" or "fakir state" because of their extremely low sliding angles and hysteresis, and we can deduce the air fraction: $f_a = (\cos(108.2) - \cos(160.4))/(1 + \cos(108.2)) = 92\%$ for $PEDOTH_{10}$ and $f_a = (\cos(110.5) - \cos(158.6))/(1 + \cos(110.5)) = 89\%$ for $PEDOTH_{12}$. The percentage of air fraction between the water droplet and the surface is thus very important in the case of $PEDOTH_{10}$ and $PEDOTH_{12}$ and explain only the extremely low hysteresis and sliding angle obtained for these surfaces.

Mechanism Discussion. If it is known that the surface morphology of electrodeposited conductive polymers highly depends on electrochemical parameters,[36,37] it is very difficult to find a correlation between surface morphology and electrochemical parameters. However, in a very recent report, the group of Berdikov studied the electrodeposition of PEDOT using various supporting electrolyte and solvent.[38] They demonstrated that the differences in surface morphology, especially observed by varying the solvent, can be explained by differences in the solubility in these solvents of EDOT oligomers electroformed during initial electropolymerization stages. More precisely, the more the insolubility of the EDOT oligomers increases, the more surface is structured.

In our work, the increase in the alkyl chain in the electropolymerization of the EDOTHn series in Bu_4NPF_6/acetonitrile has two opposite consequences: (1) it increases the insolubility of the oligomers in a polar solvent such as acetonitrile; (2) it decreases the oligomer chain length due to steric hindrances

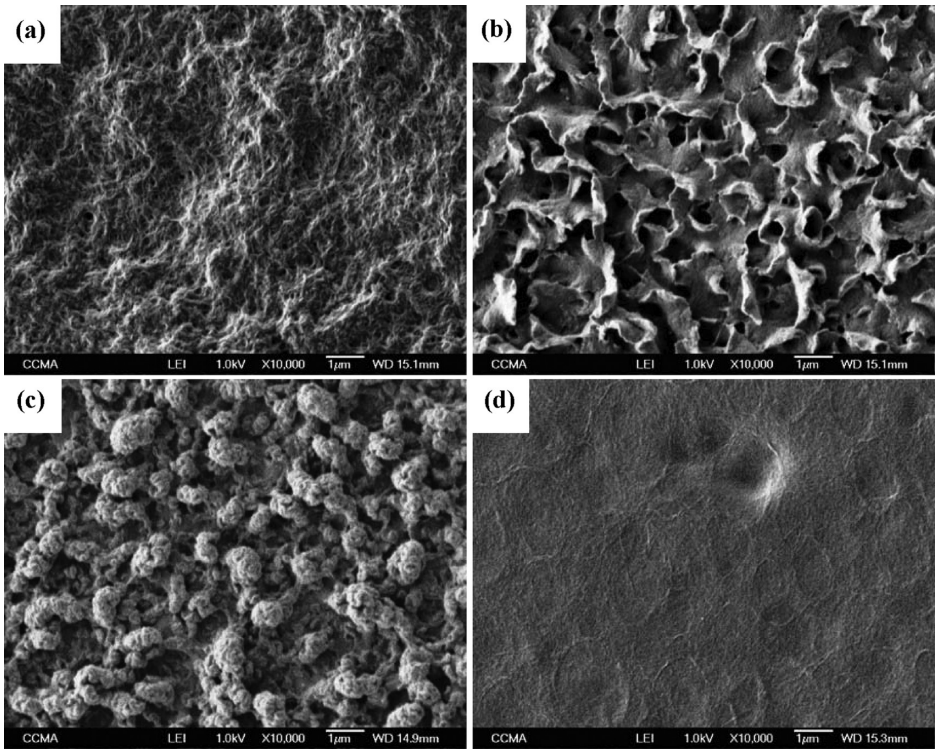

Figure 8. SEM images of $PEDOTH_{10}$ obtained with different solvents: (a) propylene carbonate, (b) benzonitrile, (c) nitrobenzene, and (d) dichloromethane (magnification ×10000; salt: Bu_4NPF_6; Q_s = 200 mC/cm^2).

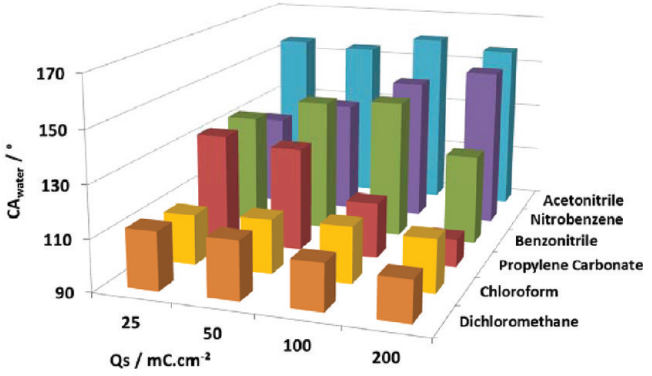

Figure 9. Static contact angles of water as a function of the solvent and the deposition charge for $PEDOTH_{10}$.

during electropolymerization and as a consequence decreases their solubility (cf. Supporting Information).

In our case the first effect seems to be more important than the second one.

In the case of the electrodeposition of $EDOTH_{10}$ in various solvent, it is evident that, due to the presence of apolar hydrocarbon chains, the $EDOTH_{10}$ oligomers should be less soluble in polar solvents such as acetonitrile, propylene carbonate, benzonitrile, and nitrobenzene (structured surfaces) than in less polar solvents such as dichloromethane or chloroform (smooth surfaces). The solvent polarity cannot explain the extreme roughness of the surface electroformed with acetonitrile because the solvent properties (dielectric constant, viscosity, basicity) may also have a very important impact on the electropolymerization and as a consequence on the polymer chain lengths.

Table 3. Influence of Chemical and Physical Parts in the Static Contact Angles (CA_{water}) of Electrodeposited Films (Solvent: Acetonitrile; Salt: Bu_4NPF_6; Q_s = 100 mC/cm^2)

		chemical part [deg/%]		
polymers	CA_{water} [deg]	polymer	doping anions	physical part [deg/%] (roughness + morphology)
$PEDOTH_{12}$	158.6	109.2/68.9	1.3/0.8	48.1/30.3
$PEDOTH_{10}$	160.4	105.7/65.9	2.5/1.6	52.2/32.5
$PEDOTH_8$	133.9	96.5/72.1	6.8/5.1	30.6/22.8
$PEDOTH_6$	98.7	80.9/82.0	17.8/18.0	0/0
$PEDOTH_4$	81.3	73.5/90.4	7.8/8.6	0/0

Superhydrophobic Surfaces by Electropolymerization of EDOT Containing Short Hydrocarbon Chain. To know if long alkyl chains are necessary to create superhydrophobic surfaces, other experiments were performed using $EDOTH_6$ as reference monomer and with other electrochemical conditions. In particular, the nature of the supporting electrolyte (one of the parameters, which impacts the more on the surface morphology)[37] has been studied. Six other supporting electrolytes were used: sodium perchlorate ($NaClO_4$), tetrabutylammonium perchlorate (Bu_4NClO_4), tetrabutylammonium tetrafluoroborate (Bu_4NBF_4), tetrabutylammonium trifluoromethanesulfonate ($Bu_4NCF_3SO_3$), tetrabutylammonium nonafluorobutanesulfonate ($Bu_4NC_4F_9SO_3$), and tetrabutylammonium heptadecafluorooctanesulfonate ($Bu_4NC_8F_{17}SO_3$). The static contact angles and the roughness parameters as a function of the supporting electrolyte and the deposition charge (Q_s = 100, 200, and 400 mC/cm^2) are given in Tables 4 and 5. First, CA_{water} above that previously

Table 4. Static Contact Angles (deg) of Water of $PEDOTH_6$ as a Function of the Salt and the Deposition Charge

Q_s [mC/cm^2]	Bu_4NPF_6	$NaClO_4$	Bu_4NClO_4	Bu_4NBF_4	$Bu_4NCF_3SO_3$	$Bu_4NC_4F_9SO_3$	$Bu_4NC_8F_{17}SO_3$
100	98.7	118.8	141.2	110.2	142.3	159.3	158.8
200	96.5	139.0	139.2	139.1	142.7	154.5	158.7
400	96.9	134.9	150.9	140.7	132.4	158.2	159.0

Table 5. Roughness Parameters (R_a/R_q) in μm of $PEDOTH_6$ as a Function of the Salt and the Deposition charge

Q_s [mC/cm^2]	Bu_4NPF_6	$NaClO_4$	Bu_4NClO_4	Bu_4NBF_4	$Bu_4NCF_3SO_3$	$Bu_4NC_4F_9SO_3$	$Bu_4NC_8F_{17}SO_3$
100	0.29/0.51	0.16/0.22	0.51/0.65	0.25/0.33	0.37/0.69	0.15/0.22	0.09/0.13
200	0.38/0.66	0.29/0.50	0.94/1.11	0.35/0.72	1.20/1.53	1.38/1.98	0.57/0.89
400		1.05/1.83	2.15/2.56	2.67/3.92	1.96/2.20	2.94/3.43	0.97/1.34

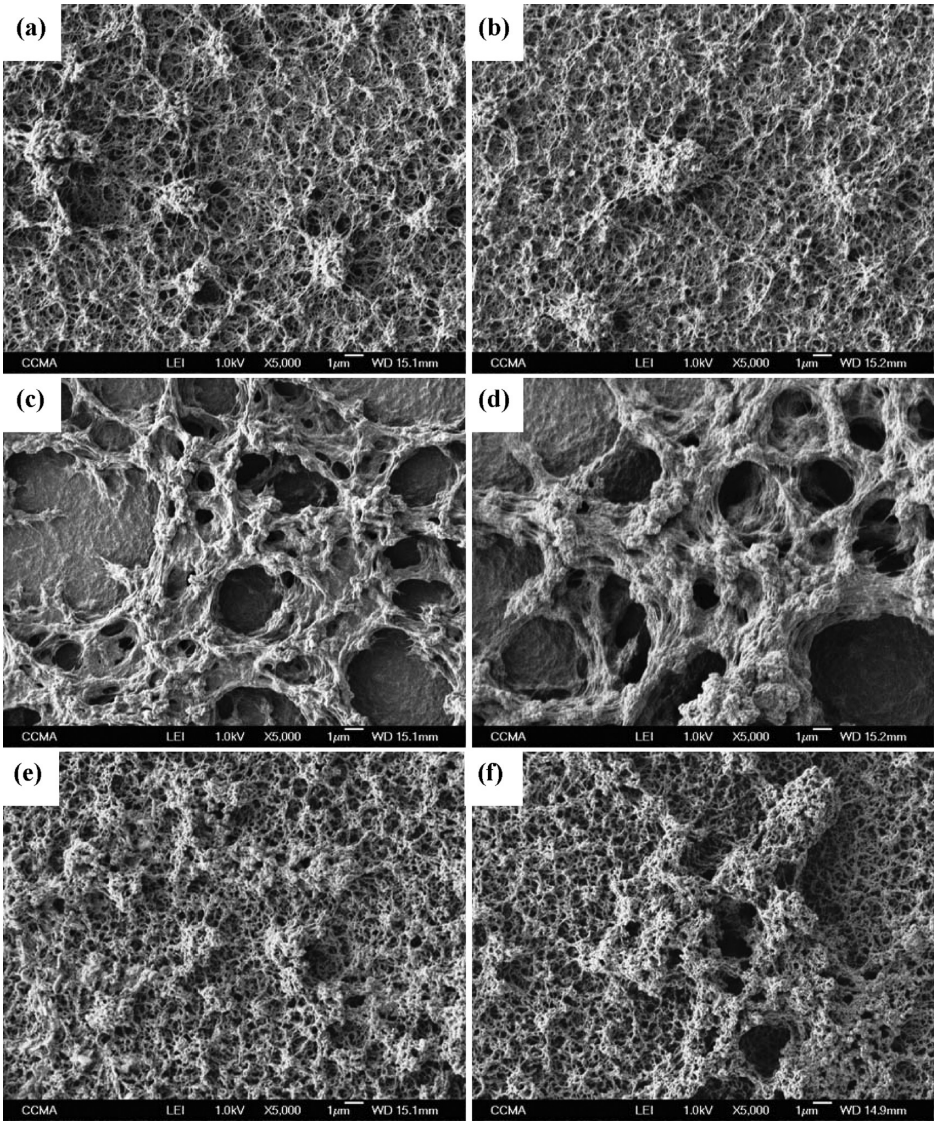

Figure 10. SEM images of $PEDOTH_6$ obtained with (a) $NaClO_4$, (b) Bu_4NClO_4, (c) Bu_4NBF_4, (d) $Bu_4NCF_3SO_3$, (e) $Bu_4NC_4F_9SO_3$, and (f) $Bu_4NC_8F_{17}SO_3$ (magnification $\times$5000; solvent: acetonitrile; Q_s = 200 mC/cm^2).

obtained with Bu_4NPF_6 were measured with all supporting electrolytes. Moreover, superhydrophobic properties were reached not only with the perfluorinated salts $Bu_4NC_4F_9SO_3$ (no sliding angle) and $Bu_4NC_8F_{17}SO_3$ (H_w = 13.9° and α_w = 11.0°) but also with Bu_4NClO_4 (no sliding angles). SEM images of the surfaces are gathered in Figure 10. A relatively

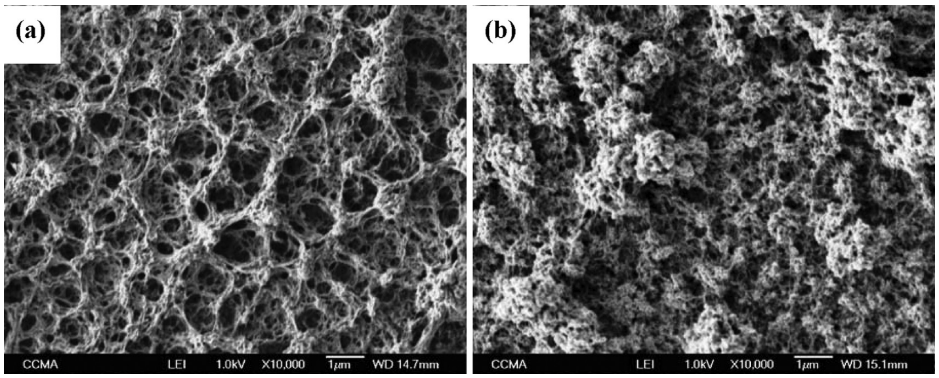

Figure 11. SEM images of PEDOT obtained with two different fluorinated salts: (a) $Bu_4NC_4F_9SO_3$ and (b) $Bu_4NC_8F_{17}SO_3$ (magnification ×10000; solvent: acetonitrile; Q_s = 200 mC/cm^2).

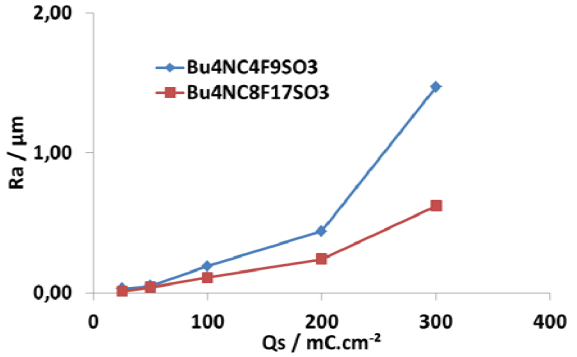

Figure 12. R_a [μm] as a function of the fluorinated salts and Q_s (monomer: EDOT).

close surface morphology was obtained with Bu_4NBF_4 and $Bu_4NCF_3SO_3$. These two surfaces were microstructured as shown in Figure 10c,d. By contrast, the surfaces elaborated with $NaClO_4$, Bu_4NClO_4, $Bu_4NC_4F_9SO_3$, and $Bu_4NC_8F_{17}SO_3$ were also nanoporous (Figure 10a,b,e,f). This surface micro/nanostructuration is expected to be better for the water-repellency properties.

Superhydrophobic Surfaces by Electropolymerization of EDOT (Nonsubstituted) Using Perfluorinated Sulfonate Salts. In this last part, we tried to determine the possibility to reach superhydrophobic surface by electrodeposition of EDOT in acetonitrile and in presence of two perfluorinated sulfonate salts ($Bu_4NC_4F_9SO_3$ or $Bu_4NC_8F_{17}SO_3$). Superhydrophobic surfaces were obtained only with $Bu_4NC_8F_{17}SO_3$ but at relatively high Q_s (CA_{water} = 150.4° for Q_s = 300 mC/cm^2) while the films obtained with $Bu_4NC_4F_9SO_3$ were hydrophilic (CA_{water} < 90° whatever Q_s). The SEM images are given in Figure 11. Structured surfaces were obtained with the two salts with very porous structures in the case of films formed with $Bu_4NC_4F_9SO_3$. Rougher surfaces were obtained with the salt containing the smaller fluorinated salt ($Bu_4NC_4F_9SO_3$), as shown in Figure 12. Hence, the films electroformed with $Bu_4NC_4F_9SO_3$ were sufficiently structured, but the polymer was not sufficiently hydrophobic due to the high polarity of sulfonate groups of perfluorinated salts.

CONCLUSIONS

In conclusion, surfaces of various wettability and morphology were elaborated by electropolymerization of EDOT derivatives containing only an alkyl (butyl, hexyl, octyl, decyl, and dodecyl) or a phenyl substituent directly grafted on the 2-position. Even if numerous publications reported the use of highly fluorinated materials (during the process or with a post-treatment), here we show that the molecular design of highly hydrocarbon materials is a sufficient way to:

- Obtain superhydrophobic surfaces at low deposition charge.
- Obtain antiwetting properties similar to that obtained with fluorinated monomers.
- Reach very competitive superhydrophobic surfaces: self-cleaning (extremely low hysteresis and sliding angle) superhydrophobic surfaces were elaborated with antiwetting surface properties similar to fluorinated analogues.
- Switch the wetting properties of a surface (hydrophilic to superhydrophobic): it was possible to switch the surface from hydrophilic to superhydrophobic by changing the alkyl chain length. Indeed, using Bu_4NPF_6 and acetonitrile as electrolyte, superhydrophobic films were obtained with *n*-$C_{12}H_{25}$ and *n*-$C_{10}H_{21}$, hydrophobic films with *n*-C_8H_{17} and *n*-C_6H_{13}, and hydrophilic with *n*-C_4H_9.
- Nucleate a double scale of surface structuration (micro and nano); the alkyl substituents not only improved the surface hydrophobicity but also participated in the surface construction (by increasing the polymer insolubility), two essential parameters for the fabrication of superhydrophobic surfaces.
- Switch from highly structured surfaces to smooth ones by changing the solvent; it is thus possible to determine the chemical and physical parts of the contact angles as well as roughness factors or air fractions.
- Reach superhydrophobic surfaces even with short alkyl chains by changing the electrochemical conditions (the nature of the supporting electrolyte, for example).
- Reach superhydrophobic surfaces without hydrocarbon chains but using perfluorinated salts and at relatively high deposition charge.

This work contributes to the elaboration of bioinspired surfaces with an ecotoxic-friendly approach and opens new perspectives within hydrocarbon series.

ASSOCIATED CONTENT

Supporting Information. Monomer characterization and electrochemical study. This material is available free of charge via the Internet at http://pubs.acs.org.

AUTHOR INFORMATION

Corresponding Author
*E-mail: Frederic.GUITTARD@unice.fr.

ACKNOWLEDGMENT

We thank Jean-Pierre Laugier of the Centre Commun de Microscopie Appliquée (CCMA) of the University of Nice Sophia Antipolis for the SEM analyses. We also thank the Provence-Alpes-Côte d' Azur (PACA) region for a research grant.

REFERENCES

(1) Zhang, X.; Shi, F.; Niu, J.; Jiang, Y.; Wang, Z. *J. Mater. Chem.* **2008**, *18*, 621–633.
(2) Roach, P.; Shirtcliffe, N. J.; Newton, M. I. *Soft Matter* **2008**, *4*, 224–240.
(3) Li, X.-M.; Reinhoudt, D.; Crego-Calama, M. *Chem. Soc. Rev.* **2007**, *36*, 1350–1368.
(4) Wenzel, R. N. *Ind. Eng. Chem.* **1936**, *28*, 988–994.
(5) Cassie, A. B. D.; Baxter, S. *Trans. Faraday Soc.* **1944**, *40*, 546–551.
(6) Baxter, S.; Cassie, A. B. D. *J. Text. Ind.* **1945**, *36*, T67–90.
(7) Öner, D.; McCarthy, T. J. *Langmuir* **2000**, *16*, 7777–7782.
(8) Lim, J.-M.; Yi, G.-R.; Moon, J. H.; Heo, C.-J.; Yang, S.-M. *Langmuir* **2007**, *23*, 7981–7989.
(9) Amigoni, S.; Taffin de Givenchy, E.; Dufay, M.; Guittard, F. *Langmuir* **2009**, *25*, 11073–11077.
(10) Qu, M.; Zhao, G.; Cao, X.; Zhang, J. *Langmuir* **2008**, *24*, 4185–4189.
(11) Bok, H.-M.; Shin, T.-Y.; Park, S. *Chem. Mater.* **2008**, *20*, 2247–2251.
(12) Zhong, W.; Wang, Y.; Yan, Y.; Sun, Y.; Deng, J.; Yang, W. *J. Phys. Chem. B* **2007**, *111*, 3918–3926.
(13) Zhu, Y.; Hu, D.; Wan, M.; Jiang, L.; Wei, Y. *Adv. Mater.* **2007**, *19*, 2092–2096.
(14) Zhu, Y.; Li, J.; Wan, M.; Jiang, L. *Macromol. Rapid Commun.* **2008**, *29*, 239–243.
(15) Wan, M. *Adv. Mater.* **2008**, *20*, 2926–2932.
(16) Zhu, Y.; Zhang, J.; Zheng, Y.; Huang, Z.; Feng, L.; Jiang, L. *Adv. Funct. Mater.* **2006**, *16*, 568–574.
(17) (a) Darmanin, T.; Guittard, F. *J. Am. Chem. Soc.* **2009**, *131*, 7928–7933. (b) Darmanin, T.; Guittard, F. *J. Mater. Chem.* **2009**, *19*, 7130–7136. (c) Darmanin, T.; Guittard, F. *J. Colloid Interface Sci.* **2009**, *335*, 146–149.
(18) (a) Zenerino, A.; Darmanin, T.; Taffin de Givenchy, E.; Amigoni, S.; Guittard, F. *Langmuir* **2010**, *26*, 13545–13549. (b) Darmanin, T.; Guittard, F.; Amigoni, S.; Taffin de Givenchy, E.; Noblin, X.; Kofman, R.; Celestini, F. *Soft Matter* **2011**, *7*, 1053–1057.
(19) (a) Darmanin, T.; Taffin de Givenchy, E.; Guittard, F. *Macromolecules* **2010**, *43*, 9365–9370. (b) Darmanin, T.; Guittard, F. *Langmuir* **2009**, *25*, 5463–5466.
(20) (a) Darmanin, T.; Taffin de Givenchy, E.; Amigoni, S.; Guittard, F. *Langmuir* **2010**, *26*, 17596–17602. (b) Darmanin, T.; Nicolas, M.; Guittard, F. *Langmuir* **2008**, *24*, 9739–9746.
(21) (a) Yan, H.; Kurogi, K.; Mayama, H.; Tsujii, K. *Angew. Chem., Int. Ed.* **2005**, *44*, 3453–3456. (b) Kurogi, K.; Yan, H.; Mayama, H.; Tsujii, K. *J. Colloid Interface Sci.* **2007**, *312*, 156–163. (c) Chiba, K.; Kurogi, K.; Monde, K.; Hashimoto, M.; Yoshida, M.; Mayama, H.; Tsujii, K. *Colloids Surf., A* **2010**, *354*, 234–239.
(22) Luo, S.-C.; Liour, S. S.; Yu, H.-H. *Chem. Commun.* **2010**, *46*, 4731–4733.
(23) (a) Xu, L.; Chen, W.; Mulchandani, A.; Yan, Y. *Angew. Chem., Int. Ed.* **2005**, *44*, 6009–6012. (b) Xu, L.; Chen, Z.; Chen, W.; Mulchandani, A.; Yan, Y. *Macromol. Rapid Commun.* **2008**, *29*, 832–838.
(24) (a) Yu, W.; Yao, T.; Xiao, L.; Wang, T.; Gao, H.; Zhang, J.; Yang, B. *J. Appl. Polym. Sci.* **2011**, *119*, 1052–1059. (b) Yan, H.; Kurogi, K.; Tsujii, K. *Colloids Surf., A* **2007**, *292*, 27–31.
(25) (a) Jiang, Y.; Wang, Z.; Yu, X.; Shi, F.; Xu, H.; Zhang, X.; Smet, M.; Dehaen, W. *Langmuir* **2005**, *21*, 1986–1990. (b) Yu, X.; Wang, Z.; Jiang, Y.; Zhang, X. *Langmuir* **2006**, *22*, 4483–4486.
(26) (a) Neinhuis, C.; Barthlott, W. *Ann. Bot.* **1997**, *79*, 667–677. (b) Barthlott, W.; Neinhuis, C. *Planta* **1997**, *202*, 1–8. (c) Wagner, T.; Neinhuis, C.; Barthlott, W. *Acta Zool.* **1996**, *77*, 213–225.
(27) (a) Gu, Z.-Z.; Wei, H.-M.; Zhang, R.-Q.; Han, G.-Z.; Pan, C.; Zhang, H.; Tian, X.-J.; Chen, Z.-M. *Appl. Phys. Lett.* **2005**, *86*, 201915/1–201915/3. (b) Shirtcliffe, N. J.; Pyatt, F. B.; Newton, M. I.; McHale, G. *J. Plant Physiol.* **2006**, *163*, 1193–1197.
(28) (a) Zheng, Y.; Gao, X.; Jiang, L. *Soft Matter* **2007**, *3*, 178–182. (b) Lee, W.; Jin, M.-K.; Yoo, W.-C.; Lee, J.-K. *Langmuir* **2004**, *20*, 7665–7669.
(29) (a) Gao, X.; Jiang, L. *Nature* **2004**, *432*, 36. (b) Parker, A. R.; Lawrence, C. R. *Nature* **2001**, *414*, 33–34.
(30) Havinga, E. E.; Mutsaers, C. M. J.; Jenneskens, L. W. *Chem. Mater.* **1996**, *8*, 769–776.
(31) (a) Kumar, A.; Welsch, D. M.; Morvant, M. C.; Piroux, F.; Abboud, K. A.; Reynolds, J. R. *Chem. Mater.* **1998**, *10*, 896–902. (b) Sankaran, B.; Reynolds, J. R. *Macromolecules* **1997**, *30*, 2582–2588.
(32) (a) Groenendaal, L.; Zotti, G.; Jonas, F. *Synth. Met.* **2001**, *118*, 105–109. (b) Breiby, D. W.; Samuelsen, E. J.; Groenendaal, L.; Struth, B. *J. Polym. Sci., Part B: Polym. Phys.* **2003**, *41*, 945–952.
(33) (a) Hollamby, M. J.; Trickett, K.; Azmi, M.; Cummings, S.; Tabor, R. F.; Myakonkaya, O.; Gold, S.; Rogers, S.; Heenan, R. K.; Eastoe, J. *Angew. Chem., Int. Ed.* **2009**, *48*, 4993–4995. (b) Eastoe, J.; Gold, S.; Steytler, D. C. *Aust. J. Chem.* **2007**, *60*, 630–632.
(34) Mohamed, A.; Trickett, K.; Chin, S. Y.; Cummings, S.; Sagisaka, M.; Hudson, L.; Nave, S.; Dyer, R.; Rogers, S. E.; Heenan, R. K.; Eastoe, J. *Langmuir* **2010**, *26*, 13861–13866.
(35) (a) Barthlott, W.; Schimmel, T.; Wiersch, S.; Koch, K.; Brede, M.; Barczewski, M.; Walheim, S.; Weis, A.; Kaltenmaier, A.; Leder, A.; Bohn, H. F. *Adv. Mater.* **2010**, *22*, 2325–2328. (b) Hosono, E.; Fujihara, S.; Honma, I.; Zhou, H. *J. Am. Chem. Soc.* **2005**, *127*, 13458–13459. (c) Yabu, H.; Takebayashi, M.; Tanaka, M.; Shimomura, M. *Langmuir* **2005**, *21*, 3235–3237.
(36) (a) Cheung, K. M.; Bloor, D.; Stevens, G. C. *Polymer* **1988**, *29*, 1709–1717. (b) Su, W.; Iroh, J. O. *Synth. Met.* **1998**, *95*, 159–167. (c) Otero, T. F.; DeLaretta, E. *Synth. Met.* **1988**, *26*, 79–88.
(37) (a) Mammone, R. J.; Binder, M. *J. Electrochem. Soc.* **1990**, *137*, 2135–2139. Wood, G. A.; Iroh, J. O. *Polym. Eng. Sci.* **1996**, *36*, 2389–2395. (c) Silk, T.; Hong, Q.; Tamm, J.; Compton, R. G. *Synth. Met.* **1998**, *93*, 59–64.
(38) Poverenov, E.; Li, M.; Bitler, A.; Bendikov, M. *Chem. Mater.* **2010**, *22*, 4019–4025.